

Prediction Model with Harmonic Load Current Components for FCS-MPC of an Uninterruptible Power Supply

Sergio Vazquez, *Fellow, IEEE*, Eduardo Zafra, *Student Member, IEEE*, Ricardo P. Aguilera, *Member, IEEE*, Tobias Geyer, *Senior Member, IEEE*, Jose I. Leon, *Fellow, IEEE*, and Leopoldo G. Franquelo, *Life Fellow, IEEE*

Abstract—A finite control set model predictive control (FCS-MPC) strategy consists of a prediction model, a cost function and an optimization algorithm. Consequently, the performance of the FCS-MPC depends on the proper design of these three elements. This paper assesses the influence of the prediction model of an uninterruptible power supply (UPS). Since the load connected to the voltage source inverter (VSI) affects the dynamic of the system state variables, the load dynamic should be included in the system model. This makes the design of the prediction model a challenge because the load connected to the VSI is generally unknown. To deal with this uncertainty, this work proposes an augmented prediction model based on a state observer that includes as many harmonic components as necessary to accurately represent the output current. The performance of the FCS-MPC for a UPS is evaluated in a laboratory prototype using the proposed and the conventional prediction models. Experimental results show that the proposed solution provides a more accurate representation of the output current, improving the system performance.

I. INTRODUCTION

FINITE control set model predictive control (FCS-MPC) is a powerful control strategy that has extensively been applied to power converters and drives in the last years [1]–[3]. This technique is considered as an advanced control strategy that provides several benefits compared to conventional solutions [4]. One of the main reasons for the success of the FCS-MPC is that the basics of the technique are easy to understand. This allows one to do an intuitive FCS-MPC design for any power conversion application [2]. In general, the designed FCS-MPC will be robust enough and provide a better system performance compared to conventional solutions even if the design criteria used are not the best [5], [6].

An FCS-MPC algorithm consists of a prediction model, a cost function and an optimization algorithm. The performance of a system governed by an FCS-MPC algorithm depends on the selected cost function, which defines the control targets, the accuracy of the prediction model to compute the future state variable values, and the ability of the optimization algorithm to compute the optimal control input within a sampling period.

The cost function is related to the particular application under consideration. Therefore, each application will use the most appropriate cost function to define the desired behavior of the state variables of interest. The cost function is composed of several terms associated with the tracking error of these state variables. A single cost function is required to control them simultaneously. Therefore, weighting factors are used to determine the relative importance of each control target [6],

[7]. The design of the most suitable cost function has been investigated for many applications like motor drives, active front ends, uninterruptible power supplies (UPSs), etc [2], [3], [8].

The optimization algorithm does not depend on the particular application, but determines the computational burden of the FCS-MPC algorithm. The computational cost is mainly determined by the length of the prediction horizon, N_p , used in FCS-MPC formulation. The prediction horizon determines the number of time steps the evolution of the state variables of interest is forecast into the future [9]. In general, long prediction horizons improve the system performance [6], [9]. The most common optimization algorithm is the exhaustive searching algorithm (ESA). The ESA evaluates the cost function for all the elements in the input control set. Then, it determines by direct comparison the one that minimizes the cost function. Considering the current development of digital control hardware platforms, this approach is suitable for short prediction horizons, $N_p \in \{1, 2\}$, [10]. However, a different strategy is necessary for long prediction horizons, $N_p \geq 3$, because the ESA is not computationally feasible for such N_p in a practical application. Solutions for dealing with this problem draw on branch and bound techniques to reduce the computational burden [11]. Among them, the sphere decoding algorithm (SDA) is a suitable solution for a practical implementation [12], [13].

The prediction model is formed by the dynamic equation of the state variables of interest. For a power conversion system, it relies on the electric circuit connected to the output of the power converter. As a consequence, it depends on the particular application. In general, it is possible to have an accurate prediction model for power conversion systems like motor drives or active front ends. The dynamic equations of the state variables for the former are related to the kind of machine [14]–[18], whereas for the latter they depend on the connection filter [19]–[22]. A common approach to deal with parameter uncertainty problems in the prediction model is the use of observer-based techniques [23]–[27]. A different approach is the model-free predictive control that make predictions of the state variable future values without using a system model. In the literature two alternatives exist. On the one hand, a system identification method, like artificial neural networks (ANN), recursive least squares (RLS) algorithm, or ultra-local model, are used to define the system behavior. Once the system is identified, this information replaces the original system model

to compute the state variable future values [28]–[30]. On the other hand, a different approach uses the system properties assuming a fast sampling period for the FCS-MPC to make the predictions of the state variable future values without using any model [31]–[33]. Although these techniques are promising, up to the authors knowledge, they have not been applied to an UPS application yet, so further research is required.

In general, model-free methods are good approaches when little or no information about the system is available. In the UPS application case, the system behavior is well represented by the output filter dynamic equations and the output load behavior. Compared to the model-free strategies, this work proposes an observer-based approach that exploits an explicitly given mathematical model of the system providing a simple and straightforward implementation.

This paper focuses on the prediction model of FCS-MPC for a UPS application. The definition of this prediction model is challenging because the output load connected to the power converter is unknown. However, the dynamic equations of the state variables depend on the output load currents. Therefore, to solve this issue, it is necessary to make some assumptions about the current load behavior, which will affect the performance of FCS-MPC. The most common approach to deal with this uncertainty is to assume that the output load current remains constant between two consecutive sampling steps [34]. This assumption relies on the high sampling frequency typically used for FCS-MPC and generally provides acceptable results. To implement this solution, the output load current can be measured, [35] or an observer can be designed to deal with system uncertainties and avoid additional sensors [34], [36].

A more precise solution is to model the characteristics of the load connected to the power converter [37]. This method provides an accurate representation of the load since no assumption about the load behavior is considered. However, in the literature this option is limited to linear loads for UPS systems [38], and for estimating the harmonics under distorted grid voltage for a grid-connected application [39]. An alternative solution is to adopt the constant load current approach and to modify the cost function to take into account the error introduced by the prediction model [40]. This procedure provides good results, especially when nonlinear loads are connected to the power converter. However, it increases the complexity of the cost function design.

The work at hands proposes a solution that takes into account that the load current is a periodical signal, independently whether the load is linear or not. Therefore, the load current can be decomposed by the sum of several harmonic components. More specifically, it is proposed to design the prediction model by using an augmented state observer that includes as many harmonic components as necessary to accurately represent the output current. This avoids the use of extra sensors, and allows the prediction model to deal with system uncertainties and any kind of output load. The augmented state observer is designed as a stationary Kalman filter. In contrast to [39], this work provide guidelines to set the values of the Kalman filter matrices, which is of high value for practical engineering. In addition, the proposed approach is also validated experimentally, including not only

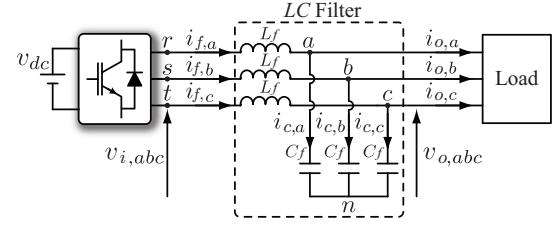


Fig. 1. Electric circuit of the UPS system under study.

TABLE I
SYSTEM VARIABLES AND PARAMETERS

Variable	Description
L_f	Output filter inductor
C_f	Output filter capacitor
$i_{f,abc} = [i_{f,a} \ i_{f,b} \ i_{f,c}]^T$	Output filter inductor current
$v_{o,abc} = [v_{o,a} \ v_{o,b} \ v_{o,c}]^T$	Output filter capacitor voltage
$v_{i,abc} = [v_{i,a} \ v_{i,b} \ v_{i,c}]^T$	VSI output voltage
v_{dc}	DC-link voltage
$S_{abc} = [S_a \ S_b \ S_c]^T$	VSI switching state
$i_{o,abc} = [i_{o,a} \ i_{o,b} \ i_{o,c}]^T$	Output load current
$v_{o,abc}^* = [v_{o,a}^* \ v_{o,b}^* \ v_{o,c}^*]^T$	Output filter capacitor reference voltage
ω	Angular frequency of the reference voltage
f_s	Sampling frequency

the steady-state performance but also the close loop transient response when the system perturbation changes, i.e., when the load connected to the UPS output terminals is modified. In Section II the system under investigation is presented and the used FCS-MPC strategy is described. Section III provides the prediction model design. The performance of FCS-MPC is evaluated in a UPS laboratory prototype using the proposed and the conventional prediction models in Section IV. The accuracy of the two approaches is compared with the help of experimental results, showing that the proposed prediction model provides a more accurate representation of the output current. In addition, the effect on the FCS-MPC performance is assessed. Finally, conclusions are drawn in Section V.

II. SYSTEM DESCRIPTION AND FCS-MPC STRATEGY

The system under study consists of a three-phase two-level voltage source inverter (VSI) with an output LC filter and an unknown load connected to the filter. The corresponding electric circuit is shown in Fig. 1. The main variables and parameters that characterize the system are summarized in Table I. In the proposed approach, the measured signals are $i_{f,abc}$ and $v_{o,abc}$, while $i_{o,abc}$ is estimated by the proposed augmented state observer. The control objective is to produce the desired sinusoidal output voltage $v_{o,abc}^*$, independently of the harmonic content of the current drawn by the output load, $i_{o,abc}$.

A. Original System Model

To analyze the system, the dynamic equations representing the system behavior are expressed in the $\alpha\beta$ stationary refer-

Fig. 2, which is a vector that characterizes the amplitude and phase of the h^{th} harmonic vector i_{oh} . Thus, the output current vector can be written as:

$$i_o = \sum_{h \in H} i_{oh} = \sum_{h \in H} e^{Jh\omega t} I_{oh}, \quad (4)$$

where

$$J = \begin{bmatrix} 0 & -1 \\ 1 & 0 \end{bmatrix}, \quad (5)$$

and

$$e^{Jh\omega t} = \begin{bmatrix} \cos(h\omega t) & -\sin(h\omega t) \\ \sin(h\omega t) & \cos(h\omega t) \end{bmatrix}, \quad (6)$$

is the rotation matrix [42]. Assuming that the components of I_{oh} are unknown constant or slowly varying signals, it is possible to compute the derivative with respect to time for each individual harmonic component as:

$$\frac{di_{oh}}{dt} = Jh\omega e^{Jh\omega t} I_{oh} = Jh\omega i_{oh}. \quad (7)$$

Expressions (4) and (7) allow one to define an augmented state space model in the time domain that takes into account the nature of the load. For instance, if one considers that the load current is composed of the non triple odd harmonics $H = \{1, -5, \dots, m\}^3$ then, the augmented state vector, the system input and output are defined as

$$x_a = [i_f^T \ v_o^T \ i_{o1}^T \ i_{o5}^T \ \dots \ i_{om}^T]^T, \quad (8)$$

$$u = v_i, \ y = [i_f^T \ v_o^T]^T, \quad (9)$$

respectively, leading to the following augmented state space system:

$$\frac{dx_a}{dt} = A_{ac}x_a + B_{ac}u + \varpi \quad (10)$$

$$y = C_{ac}x_a + \nu \quad (11)$$

in which

$$A_{ac} = \begin{bmatrix} O_2 & -\frac{1}{L_f}I_2 & O_2 & O_2 & \dots & O_2 \\ \frac{1}{C_f}I_2 & O_2 & -\frac{1}{C_f}I_2 & -\frac{1}{C_f}I_2 & \dots & -\frac{1}{C_f}I_2 \\ O_2 & O_2 & J\omega & O_f & \dots & O_2 \\ O_2 & O_2 & O_2 & -J5\omega & \dots & O_2 \\ \vdots & \vdots & \vdots & \vdots & \ddots & \vdots \\ O_2 & O_2 & O_2 & O_2 & \dots & Jm\omega \end{bmatrix} \quad (12)$$

$$B_{ac} = \begin{bmatrix} \frac{1}{L_f}I_2 \\ O_2 \\ O_2 \\ O_2 \\ \vdots \\ O_2 \end{bmatrix}, \quad C_{ac} = \begin{bmatrix} I_2 & O_2 & O_2 & O_2 & \dots & O_2 \\ O_2 & I_2 & O_2 & O_2 & \dots & O_2 \end{bmatrix}. \quad (13)$$

are the continuous time plant matrices, with I_2 and O_2 representing identity and zero matrices of dimension 2×2 , respectively.

³Note that each particular harmonic is a positive- or negative-sequence vector [43]. For instance, the 5^{th} harmonic component is a negative-sequence vector rotating at -5ω , thus it is represented using $h = -5$.

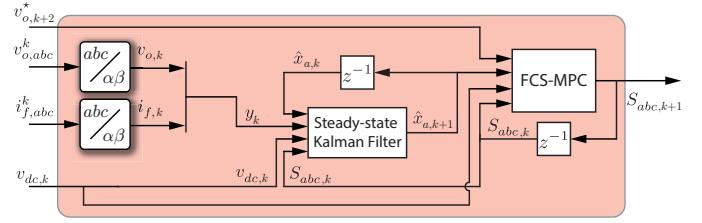


Fig. 3. Block diagram of the proposed control strategy.

This system can be discretized by using the exact Euler discretization method and is proposed to be used as the new prediction model for FCS-MPC as:

$$x_{a,k+1} = A_a x_{a,k} + B_a u_k + \varpi_k \quad (14)$$

$$y_k = C_a x_{a,k} + \nu_k, \quad (15)$$

where A_a , B_a and C_a are the resulting matrices after applying the exact Euler discretization method to the continuous-time plant (10)-(11). However, to take full advantage of this model, it is required to know all the harmonic components in the load current i_{oh} . Because these values cannot be directly measured, an observer is designed to address this issue. The observer can be formulated in the discrete domain as [44], [45]:

$$\hat{x}_{a,k+1} = A_a \hat{x}_{a,k} + B_a u_k + G_{obs} (y_k - \hat{y}_k) \quad (16)$$

$$\hat{y}_k = C_a \hat{x}_{a,k}, \quad (17)$$

where $\hat{x}_{a,k}$ and $\hat{x}_{a,k+1}$ are the augmented state estimates at time step k and $k+1$, respectively, u_k represents the augmented system input at time step k and it is calculated as in (2) and \hat{y}_k is the augmented system output estimate at the time step k .

The last step is to design the observer gain matrix G_{obs} so that the closed-loop observer matrix $A_{obs} = A_a - G_{obs}C_a$ is Schur stable⁴. This can be done considering the observer (16)-(17) as a steady-state Kalman filter [41]. Thus, the matrix G_{obs} can be computed as the following Riccati equation:

$$G_{obs} = A_a P C_a^T (C_a P C_a^T + R_f)^{-1} \quad (18a)$$

$$P = A_a P A_a^T - G_{obs} C_a P A_a^T + Q_f, \quad (18b)$$

where P is the steady-state estimate covariance matrix, and R_f and Q_f denote the measurement and process noise covariance matrices. On one hand, the measurement noise covariance matrix is related to the current and voltage sensor covariance. It is reasonable to assume that all current sensors and voltage sensors have the same covariance r_i and r_v , respectively. These values depend on the experimental setup and can be computed by recording a large number of measurements from each sensor fed with a constant input value and computing the covariance of the data set. Then, the matrix R_f can be defined as:

$$R_f = \begin{bmatrix} r_i I_2 & O_2 \\ O_2 & r_v I_2 \end{bmatrix}. \quad (19)$$

On the other hand, the process noise covariance matrix is related to unmodeled or wrongly modeled state dynamics

⁴A square matrix $A \in \mathbb{R}^{n \times n}$ is said to be Schur stable if all eigenvalues of A have norm strictly less than one [46].



Fig. 4. Test bench: (a) VSI and LC filter, (b) LC filter and voltage and current sensors, (c) non-linear load and, (d) control hardware and user interface.

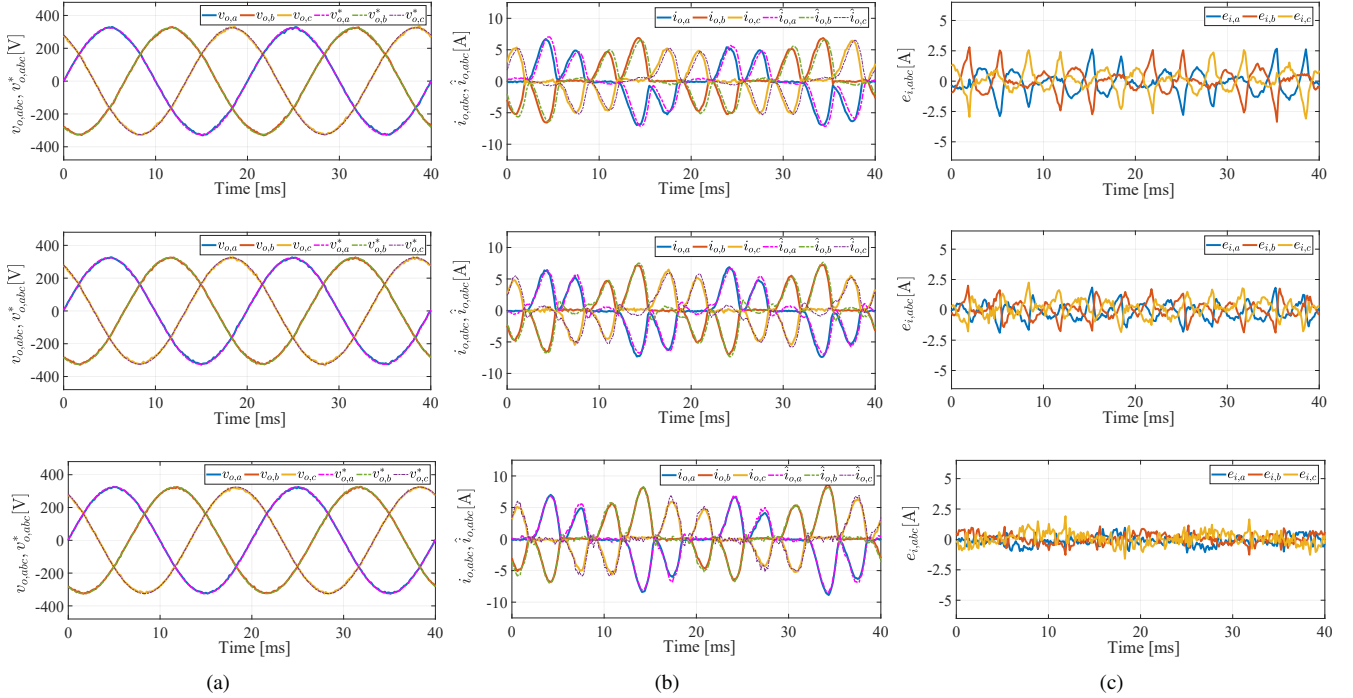


Fig. 5. Output filter capacitor voltage, output load current and current estimation error in the steady-state when the proposed prediction model is used: (a) From top to bottom: Output voltage with $H = \{1\}$, $H = \{1, -5\}$ and $H = \{1, -5, 7, -11, 13\}$, (b) from top to bottom: Load current with $H = \{1\}$, $H = \{1, -5\}$ and $H = \{1, -5, 7, -11, 13\}$ and (c) from top to bottom: Current estimation error $e_{i,j} = (i_{o,j} - \hat{i}_{o,j})_{j=a,b,c}$ with $H = \{1\}$, $H = \{1, -5\}$ and $H = \{1, -5, 7, -11, 13\}$.

in the state space model. Since the electric model for this circuit does reflect quite well the system dynamics, the process covariance can be chosen as:

$$Q_f = q_f I_n \quad (20)$$

where, q_f is a small positive scalar value and I_n is the identity matrix with dimension $n \times n$ with n equal to the order of the vector $\hat{x}_{a,k}$. Note that for a given measurement covariance matrix R_f , smaller values of q_f will imply that the system model is almost perfect. Thus, the observer will tend to rely more on predictions rather than measurements. Conversely, larger values of q_f will imply that the observer will rely more on the output measurements. However, this will increase the amount of noise coming from sensors that is transferred to the estimated states. Consequently, this tuning parameter can be used to choose the resulting observer bandwidth. Once R_f and Q_f are defined, inserting (18a) into (18b) allows one to compute P as the solution to the discrete-time algebraic Riccati equation [41]. Once P is computed, G_{obs} can be determined from (18a). Note that P and G_{obs} are time-invariant matrices.

Therefore, they can be computed off-line avoiding the increase of the computational burden during real time implementation, e.g., using the *idare* function in MATLAB. Alternatively, an autocovariance least-squares (ALS) method can be used to tune the covariance matrices Q_f and R_f ; see, e.g., [47], [48]. However, an ALS method requires extra calculations since they need to be computed online at each sampling instant.

A block diagram for the proposed control and observer structure is depicted in Fig. 3. At time step k the dc-link voltage and the output filter voltage and current are measured. The system output vector y_k can be calculated by transforming the variables $v_{o,abc}^k$ and $i_{f,abc}^k$ to the $\alpha\beta$ frame. The system input u_k is defined by the dc-link voltage measurement $v_{dc,k}$ and the optimal switching state $S_{abc,k}$ calculated in the previous iteration of the algorithm which is applied in the current sampling interval. This information is used to compute the augmented state estimate $\hat{x}_{a,k+1}$ by using the proposed augmented state observer (16)-(17). Finally, the FCS-MPC determines the optimal control action $S_{abc,k+1}$ for the time step $k+1$ by using the prediction model (14)-(15) to compute

TABLE III
PARAMETERS FOR EXPERIMENTS

Parameters	Value
Output filter inductor, L_f	2 mH
Output filter capacitor, C_f	50 μ F
Rectifier filter inductor, L_r	2 mH
Rectifier output capacitor, C_r	2200 μ F
DC load resistor	180 Ω
DC-link voltage, v_{dc}	700 V
Voltage reference (phase to ground)	230 V
Fundamental frequency	50 Hz
Sampling frequency, f_s	40 kHz
Weighting factor, λ	1.5
Kalman filter tuning parameter, q_f	0.0001

the output filter voltage prediction values at time step $k+2$ for each possible switching state and minimizing the cost function (3).

IV. EXPERIMENTAL RESULTS

In this section, the effectiveness of the proposed prediction model is verified in the test bench depicted in Fig. 4. Two experimental tests are conducted. The first one investigates the effect of considering a different number of harmonic components in the prediction model when a nonlinear load is connected to the UPS output. The second test compares the system performance when the conventional prediction model in [34] and the proposed one are used to control the output voltage applied to a diode rectifier.

The proposed FCS-MPC is implemented on the Pynq-Z1 evaluation board, which is a Xilinx system on a chip Zynq-7000-based control hardware platform. The system parameters for the experiments are summarized in Table III. The weighting factor λ value is chosen to limit the average switching frequency produced by the FCS-MPC. The value is set heuristically in the experiments in order to achieve an average switching frequency of 5 kHz. In addition, the Kalman filter tuning parameter q_f is designed to provide an observer bandwidth of roughly 1 kHz. Note that the observer bandwidth is computed calculating the natural frequency of the slowest pole of the resulting closed-loop observer matrix A_{obs} . Finally, the output filter inductor current and capacitor voltage sensor covariances are $r_i = 0.0009$ and $r_v = 0.06$, respectively.

A. Assessment of the Proposed Prediction Model Design

The first experimental test evaluates the influence of the number of harmonics considered in the prediction model. The output capacitor voltage, load current, output current estimate waveform and current estimation error are presented in Fig. 5 for $H = \{1\}$, $H = \{1, -5\}$ and $H = \{1, -5, 7, -11, 13\}$. Increasing the number of harmonics in H provides a more accurate output current estimate. Particularly, the phase shift between the actual and the estimate current is removed, allowing the observer to properly track the actual load current. Improving the observer accuracy allows FCS-MPC to increase

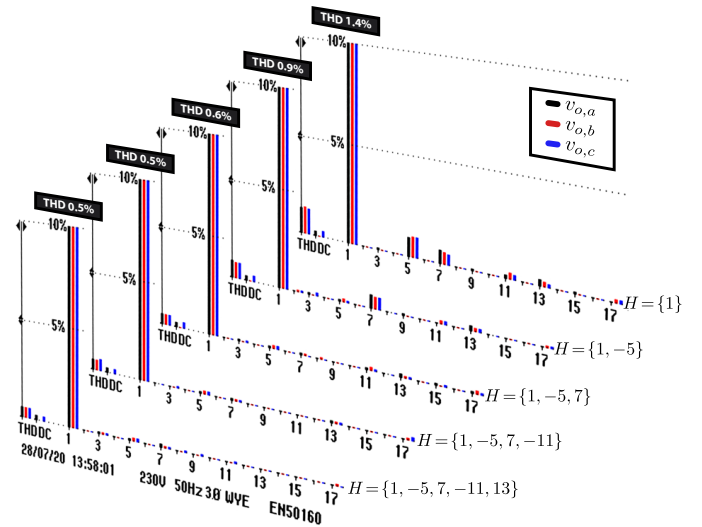


Fig. 6. Output voltage harmonic spectrum for different number of harmonic components in the prediction model.

its performance. This statement is confirmed when the total harmonic distortion (THD) and the harmonic spectrum of the output capacitor voltage are analyzed. Fig. 6 shows how these characteristics change as the number of harmonics in H increases. Clearly, FCS-MPC is able to compensate a particular harmonic when such harmonic order is included in the observer. Based on these results, it is also concluded that low order harmonics have more influence on the observer performance than high order ones. In addition, experiments show that when a low order harmonic is included in the observer not only this particular harmonic is compensated but also the high order ones. For instance, Fig. 6 shows that when $H = \{1, -5\}$ the 11th and 13th harmonic content are smaller compared to the case $H = \{1\}$. The additional information about the low order harmonic content of the output current provided by the observer reduces FCS-MPC control effort needed to compensate its effect, allowing FCS-MPC to focus on the higher order components. Therefore, as higher order harmonic content is small in general, a limited number of harmonics in H is enough to provide a good closed-loop performance. This is particularly important to limit the computational burden of the algorithm. It is important to highlight that the average switching frequency is 5 kHz in all the experiments independently of the number of harmonics in H . Therefore, the system performance is improved without increasing the switching losses.

B. Conventional vs Proposed Prediction Model

Once the performance of the proposed model is assessed, it is convenient to compare its performance against the conventional solution. The most common approach to estimate the output load current is to assume that $i_{o,k+1} = i_{o,k}$ [34]. To assess the controller performance both the transient and the steady-state responses are evaluated. Fig. 7 shows the transient response for both prediction model approaches when the load is suddenly connected to the UPS output terminals.

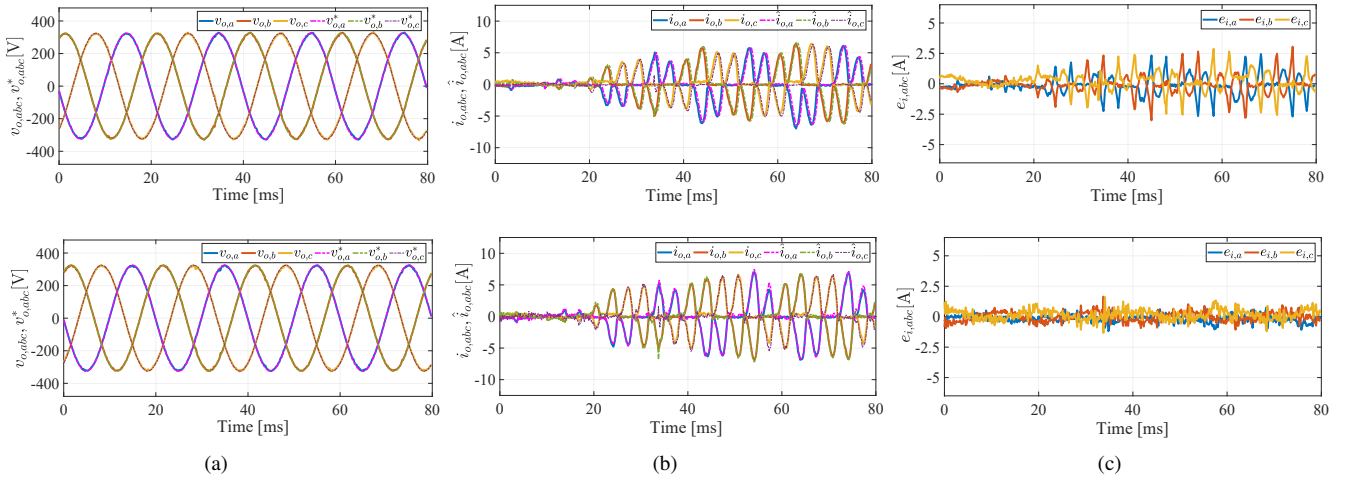


Fig. 7. Output filter capacitor voltage, output load current and current estimation error. Top represents transient response when the conventional prediction model [34] is used and, bottom shows transient result when the proposed prediction model is employed with $H = \{1, -5, 7, -11, 13\}$. (a) Output voltage, (b) load current and (c) current estimation error.

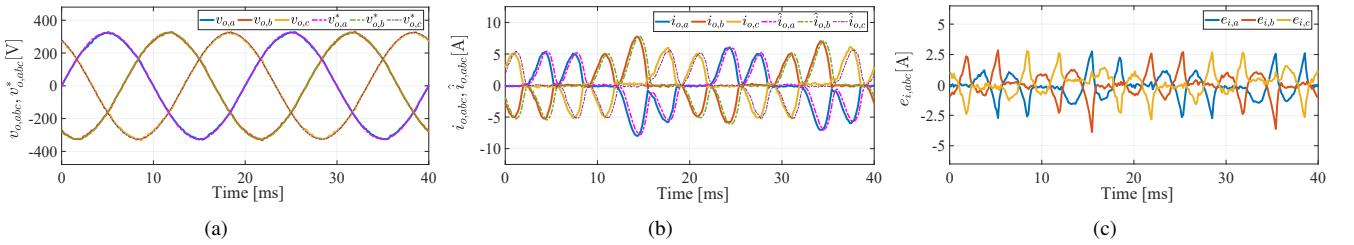


Fig. 8. Output filter capacitor voltage and output load current in the steady-state when the conventional prediction model [34] is used: (a) Output voltage, (b) load current and (c) current estimation error.

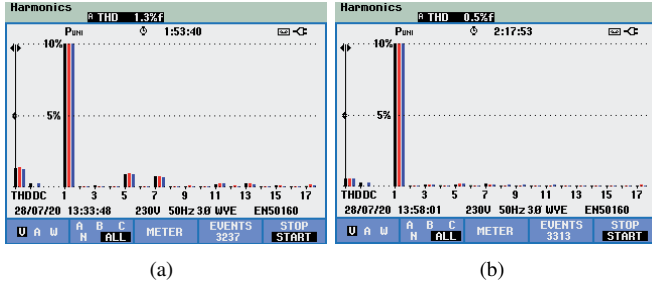


Fig. 9. Spectrum of the output voltage: (a) Conventional prediction model [34] and (b) proposed prediction model $H = \{1, -5, 7, -11, 13\}$.

The comparison of both performances allows one to conclude that the proposed observer maintains the dynamic response compared to the conventional solution. Fig. 8 shows the output capacitor voltage, load current, output current estimate and current estimation error at steady-state for the conventional solution. This observer provides a good estimate but the phase shift between the actual and the estimated current is noticeable. As a consequence, FCS-MPC is not able to compensate the effect of the low order harmonic components in the output current. This affects to the harmonic spectrum of the output capacitor voltage, where these low order harmonics are present in Fig. 9(a). Clearly, the harmonic spectrum in Fig. 9(b) when the proposed prediction model is used with

$H = \{1, -5, 7, -11, 13\}$ is better. In addition, the proposed prediction model reduces the THD from 1.3 % to 0.5 %. Finally, the computational cost for both controllers are measured in the control hardware. The conventional solution needs $12.62 \mu\text{s}$ to complete the algorithm computation while the proposed approach takes $14.99 \mu\text{s}$, which is not a significant difference for the current state-of-the-art control hardware platforms. Therefore, it can be concluded that the new proposal performs better than the conventional solution.

V. CONCLUSION AND FUTURE WORK

This paper studies the influence an observer-based prediction model has on the closed-loop performance of an FCS-MPC strategy governing a UPS system. This problem is challenging due to the lack of information about the load connected to the UPS output terminals. Conventional solution relies on the fact that FCS-MPC uses a high sampling frequency, assuming thus that the output current is almost constant from one sampling instant to the next one. Experimental results show that with this approach FCS-MPC only compensates high order harmonic components in the load, but does not properly take care of low order harmonics due to the lack of this information in the prediction model. In contrast, in this paper it is proposed to consider the fact that the load current is a periodical signal, which is composed of the sum of different harmonics, to design the prediction model. This

key idea is used to develop a steady-state Kalman filter to estimate the output current, providing the low order harmonic content information of the output load to the prediction model. Experimental results show that this new approach allows FCS-MPC to compensate not only high but also low order harmonic components in the load when they are included in the model. These results also show that due to the ability of FCS-MPC to compensate high order harmonic content, it is not necessary to include a large number of harmonics in the prediction model to achieve a high performance. This is particularly important to limit the computational burden of the algorithm. In addition, the proposed prediction model does not modify the average switching frequency of FCS-MPC. Thus, performance is improved while keeping the switching losses in the same range. Finally, the comparative experimental results for the proposed and conventional solutions allow one to conclude that the proposed approach is more suitable for a UPS application than the conventional one. Improving the accuracy of the output load estimate increases the system performance by lowering the THD of the generated output voltage, which is reduced from 1.3 % to 0.5 %, i.e., by 61.5 %.

Future research direction should address the use of different approaches to deal with parameter and load uncertainties, like model-free FCS-MPC (MF-FCS-MPC) for UPS system. MF-FCS-MPC based on system identification methods or difference detection techniques have shown promising results for other applications. Therefore, studies should investigate both alternatives. Besides the controller design, robustness and stability for this approach should be analyzed in detail for the UPS application, where the resonant frequency of the output LC filter can produce instabilities in the system.

REFERENCES

- [1] S. Kouro, P. Cortes, R. Vargas, U. Ammann, and J. Rodriguez, "Model predictive control—a simple and powerful method to control power converters," *IEEE Transactions on Industrial Electronics*, vol. 56, no. 6, pp. 1826–1838, June 2009.
- [2] S. Vazquez, J. I. Leon, L. G. Franquelo, J. Rodriguez, H. A. Young, A. Marquez, and P. Zanchetta, "Model predictive control: A review of its applications in power electronics," *IEEE Industrial Electronics Magazine*, vol. 8, no. 1, pp. 16–31, March 2014.
- [3] S. Vazquez, J. Rodriguez, M. Rivera, L. G. Franquelo, and M. Norambuena, "Model predictive control for power converters and drives: Advances and trends," *IEEE Transactions on Industrial Electronics*, vol. 64, no. 2, pp. 935–947, Feb 2017.
- [4] T. Dragicevic, S. Vazquez, and P. Wheeler, "Advanced control methods for power converters in dg systems and microgrids," *IEEE Transactions on Industrial Electronics*, pp. 1–1, 2020.
- [5] P. Karamanakos, T. Geyer, and R. Kennel, "On the choice of norm in finite control set model predictive control," *IEEE Transactions on Power Electronics*, vol. 33, no. 8, pp. 7105–7117, Aug 2018.
- [6] P. Karamanakos and T. Geyer, "Guidelines for the design of finite control set model predictive controllers," *IEEE Transactions on Power Electronics*, vol. 35, no. 7, pp. 7434–7450, July 2020.
- [7] P. Cortes, S. Kouro, B. La Rocca, R. Vargas, J. Rodriguez, J. I. Leon, S. Vazquez, and L. G. Franquelo, "Guidelines for weighting factors design in model predictive control of power converters and drives," in *2009 IEEE International Conference on Industrial Technology*, Feb 2009, pp. 1–7.
- [8] J. Rodriguez, M. P. Kazmierkowski, J. R. Espinoza, P. Zanchetta, H. Abu-Rub, H. A. Young, and C. A. Rojas, "State of the art of finite control set model predictive control in power electronics," *IEEE Transactions on Industrial Informatics*, vol. 9, no. 2, pp. 1003–1016, May 2013.
- [9] C. Bordons and C. Montero, "Basic principles of mpc for power converters: Bridging the gap between theory and practice," *IEEE Industrial Electronics Magazine*, vol. 9, no. 3, pp. 31–43, Sep. 2015.
- [10] S. Kouro, M. A. Perez, J. Rodriguez, A. M. Llor, and H. A. Young, "Model predictive control: Mpc's role in the evolution of power electronics," *IEEE Industrial Electronics Magazine*, vol. 9, no. 4, pp. 8–21, Dec 2015.
- [11] P. Karamanakos, T. Geyer, N. Oikonomou, F. D. Kieferndorf, and S. Manias, "Direct model predictive control: A review of strategies that achieve long prediction intervals for power electronics," *IEEE Industrial Electronics Magazine*, vol. 8, no. 1, pp. 32–43, March 2014.
- [12] T. Geyer and D. E. Quevedo, "Multistep finite control set model predictive control for power electronics," *IEEE Transactions on Power Electronics*, vol. 29, no. 12, pp. 6836–6846, Dec 2014.
- [13] P. Acuna, C. A. Rojas, R. Baidya, R. P. Aguilera, and J. E. Fletcher, "On the impact of transients on multistep model predictive control for medium-voltage drives," *IEEE Transactions on Power Electronics*, vol. 34, no. 9, pp. 8342–8355, 2019.
- [14] T. Geyer, G. Papafotiou, and M. Morari, "Model predictive direct torque control—part i: Concept, algorithm, and analysis," *IEEE Transactions on Industrial Electronics*, vol. 56, no. 6, pp. 1894–1905, June 2009.
- [15] H. Miranda, P. Cortes, J. I. Yuz, and J. Rodriguez, "Predictive torque control of induction machines based on state-space models," *IEEE Transactions on Industrial Electronics*, vol. 56, no. 6, pp. 1916–1924, June 2009.
- [16] C. A. Rojas, J. I. Yuz, C. A. Silva, and J. Rodriguez, "Comments on "predictive torque control of induction machines based on state-space models"," *IEEE Transactions on Industrial Electronics*, vol. 61, no. 3, pp. 1635–1638, March 2014.
- [17] M. Preindl and S. Bolognani, "Model predictive direct torque control with finite control set for pmsm drive systems, part 2: Field weakening operation," *IEEE Transactions on Industrial Informatics*, vol. 9, no. 2, pp. 648–657, May 2013.
- [18] —, "Model predictive direct torque control with finite control set for pmsm drive systems, part 1: Maximum torque per ampere operation," *IEEE Transactions on Industrial Informatics*, vol. 9, no. 4, pp. 1912–1921, Nov 2013.
- [19] S. Vazquez, A. Marquez, R. Aguilera, D. Quevedo, J. I. Leon, and L. G. Franquelo, "Predictive optimal switching sequence direct power control for grid-connected power converters," *IEEE Transactions on Industrial Electronics*, vol. 62, no. 4, pp. 2010–2020, April 2015.
- [20] S. Vazquez, P. Acuna, R. P. Aguilera, J. Pou, J. I. Leon, and L. G. Franquelo, "Dc-link voltage-balancing strategy based on optimal switching sequence model predictive control for single-phase h-npc converters," *IEEE Transactions on Industrial Electronics*, vol. 67, no. 9, pp. 7410–7420, Sep. 2020.
- [21] H. Miranda, R. Teodorescu, P. Rodriguez, and L. Helle, "Model predictive current control for high-power grid-connected converters with output lcl filter," in *2009 35th Annual Conference of IEEE Industrial Electronics*, Nov 2009, pp. 633–638.
- [22] N. Panten, N. Hoffmann, and F. W. Fuchs, "Finite control set model predictive current control for grid-connected voltage-source converters with lcl filters: A study based on different state feedbacks," *IEEE Transactions on Power Electronics*, vol. 31, no. 7, pp. 5189–5200, July 2016.
- [23] S. A. Davari, D. A. Khaburi, F. Wang, and R. M. Kennel, "Using full order and reduced order observers for robust sensorless predictive torque control of induction motors," *IEEE Transactions on Power Electronics*, vol. 27, no. 7, pp. 3424–3433, July 2012.
- [24] J. Wang, F. Wang, Z. Zhang, S. Li, and J. Rodríguez, "Design and implementation of disturbance compensation-based enhanced robust finite control set predictive torque control for induction motor systems," *IEEE Transactions on Industrial Informatics*, vol. 13, no. 5, pp. 2645–2656, Oct 2017.
- [25] L. Yan, F. Wang, M. Dou, Z. Zhang, R. Kennel, and J. Rodríguez, "Active disturbance-rejection-based speed control in model predictive control for induction machines," *IEEE Transactions on Industrial Electronics*, vol. 67, no. 4, pp. 2574–2584, April 2020.
- [26] C. Xia, M. Wang, Z. Song, and T. Liu, "Robust model predictive current control of three-phase voltage source pwm rectifier with online disturbance observation," *IEEE Transactions on Industrial Informatics*, vol. 8, no. 3, pp. 459–471, Aug 2012.
- [27] Z. Song, C. Xia, and T. Liu, "Predictive current control of three-phase grid-connected converters with constant switching frequency for wind energy systems," *IEEE Transactions on Industrial Electronics*, vol. 60, no. 6, pp. 2451–2464, June 2013.

- [28] Y. Zhang, J. Jin, and L. Huang, "Model-free predictive current control of pmsm drives based on extended state observer using ultralocal model," *IEEE Transactions on Industrial Electronics*, vol. 68, no. 2, pp. 993–1003, 2021.
- [29] J. Rodríguez, R. Heydari, Z. Rafiee, H. A. Young, F. Flores-Bahamonde, and M. Shahparasti, "Model-free predictive current control of a voltage source inverter," *IEEE Access*, vol. 8, pp. 211 104–211 114, 2020.
- [30] S. Sabzevari, R. Heydari, M. Mohiti, M. Savaghebi, and J. Rodriguez, "Model-free neural network-based predictive control for robust operation of power converters," *Energies*, vol. 14, no. 8, 2021. [Online]. Available: <https://www.mdpi.com/1996-1073/14/8/2325>
- [31] C.-K. Lin, T.-H. Liu, J.-t. Yu, L.-C. Fu, and C.-F. Hsiao, "Model-free predictive current control for interior permanent-magnet synchronous motor drives based on current difference detection technique," *IEEE Transactions on Industrial Electronics*, vol. 61, no. 2, pp. 667–681, 2014.
- [32] Y. Zhang and J. Liu, "An improved model-free predictive current control of pwm rectifiers," in *2017 20th International Conference on Electrical Machines and Systems (ICEMS)*, 2017, pp. 1–5.
- [33] V.-T. Le and H.-H. Lee, "An enhanced model-free predictive control to eliminate stagnant current variation update for pwm rectifiers," *IEEE Journal of Emerging and Selected Topics in Power Electronics*, pp. 1–1, 2021.
- [34] P. Cortes, G. Ortiz, J. I. Yuz, J. Rodriguez, S. Vazquez, and L. G. Franquelo, "Model predictive control of an inverter with output lc filter for ups applications," *IEEE Transactions on Industrial Electronics*, vol. 56, no. 6, pp. 1875–1883, June 2009.
- [35] T. Dragičević and M. Novak, "Weighting factor design in model predictive control of power electronic converters: An artificial neural network approach," *IEEE Transactions on Industrial Electronics*, vol. 66, no. 11, pp. 8870–8880, Nov 2019.
- [36] P. Mattavelli, "An improved deadbeat control for ups using disturbance observers," *IEEE Transactions on Industrial Electronics*, vol. 52, no. 1, pp. 206–212, Feb 2005.
- [37] S. Vazquez, A. Marquez, J. I. Leon, L. G. Franquelo, and T. Geyer, "Fcs-mpc and observer design for a vsi with output lc filter and sinusoidal output currents," in *2017 11th IEEE International Conference on Compatibility, Power Electronics and Power Engineering (CPE-POWERENG)*, April 2017, pp. 677–682.
- [38] E. Zafra, S. Vazquez, T. Geyer, F. J. González, A. Marquez, J. I. Leon, and L. G. Franquelo, "Finite control set model predictive control with an output current observer in the dq-synchronous reference frame for an uninterruptible power supply system," in *2019 IEEE 13th International Conference on Compatibility, Power Electronics and Power Engineering (CPE-POWERENG)*, April 2019, pp. 1–6.
- [39] C. Fischer, S. Mariéthoz, and M. Morari, "A model predictive control approach to reducing low order harmonics in grid inverters with lcl filters," in *IECON 2013 - 39th Annual Conference of the IEEE Industrial Electronics Society*, 2013, pp. 3252–3257.
- [40] B. Majmunović, T. Dragičević, and F. Blaabjerg, "Multi objective modulated model predictive control of stand-alone voltage source converters," *IEEE Journal of Emerging and Selected Topics in Power Electronics*, pp. 1–1, 2019.
- [41] G. C. Goodwin, S. F. Graebe, and M. E. Salgado, *Control System Design*, P. Hall, Ed., Upper Saddle River, New Jersey, 2001.
- [42] G. Escobar, A. M. Stankovic, and P. Mattavelli, "An adaptive controller in stationary reference frame for D-statcom in unbalanced operation," *IEEE Transactions on Industrial Electronics*, vol. 51, no. 2, pp. 401–409, 2004.
- [43] S. Vazquez, J. A. Sanchez, M. R. Reyes, J. I. Leon, and J. M. Carrasco, "Adaptive vectorial filter for grid synchronization of power converters under unbalanced and/or distorted grid conditions," *IEEE Transactions on Industrial Electronics*, vol. 61, no. 3, pp. 1355–1367, 2014.
- [44] B. D. O. Anderson and J. B. Moore, *Optimal Filtering*, N. Prentice-Hall, Englewood Cliffs, Ed., 1979.
- [45] G. Ellis, *Observers in Control Systems A Practical Guide*, A. Press, Ed., 2002.
- [46] R. Bhatia, *Matrix Analysis*, 1st ed., ser. 169. Springer-Verlag New York, 1997.
- [47] B. J. Odelson, M. R. Rajamani, and J. B. Rawlings, "A new autocovariance least-squares method for estimating noise covariances," *Automatica*, vol. 42, no. 2, pp. 303–308, 2006.
- [48] J. Rodas, C. Martín, M. R. Arahal, F. Barrero, and R. Gregor, "Influence of covariance-based ALS methods in the performance of predictive controllers with rotor current estimation," *IEEE Transactions on Industrial Electronics*, vol. 64, no. 4, pp. 2602–2607, 2017.